Diagnostic and Interventional Imaging (2019) **100**, 763—770

ORIGINAL ARTICLE /*Medical physics*

Noise assessment across two generations of iterative reconstruction algorithms of three manufacturers using bone reconstruction kernel

J. Greffier*, J. Frandon, A. Larbi, D. Om, J.P. Beregi, F. Pereira

EA 2415, Department of Radiology, Medical Imaging Group Nîmes, University of Montpellier, CHU Nîmes, boulevard du Professeur Robert Debré, 30029 Nîmes cedex, France

KEYWORDS
Multidetector computed tomography;
Image quality enhancement;
Iterative reconstruction;
Optimization;
Noise power spectrum

Abstract
Purpose: To compare the noise-magnitude and noise-texture obtained using strong kernel across two generations of iterative reconstruction (IR) algorithms proposed by three manufacturers.
Materials and methods: Five computed tomography (CT) systems equipped with two generations of IR algorithm (hybrid/statistical IR [H/SIR] or full/partial model-based IR [MBIR]) were compared. Acquisitions on Catphan 600 phantom were performed at 120 kV and three dose levels ($CTDI_{vol}$: 3, 7 and 12mGy). Raw data were reconstructed using standard ''bone'' kernel for filtered back projection and one iterative level of two generations of IR algorithms. Contrast-to-noise ratio (CNR) was computed using three regions of interest placed semi-automatically: two placed in the low-density polyethylene and Teflon inserts and another placed on the solid water. Noise power spectrum (NPS) was computed to assess the NPS-peak and noise-texture.
Results: CNR was significantly greater in MBIR compared to H/SIR algorithms for all CT systems ($P < 0.01$). CNR were improved on average from H/SIR to MBIR of 36 ± 14% [SD] (range: 24—57%) for GE-Healthcare, 109 ± 19 [SD] % (range: 89—139%) for Philips Healthcare and 42 ± 5 [SD] % (range: 36—47%) for Siemens Healthineers. The mean NPS peak decreased from H/SIR to MBIR by -41 ± 6 [SD] % (range: −47—−35%) for GE Healthcare, -79 ± 3 [SD] % (range: −82—−76%) for Philips Healthcare and -52 ± 2 [SD] % (range: −54—−51%) for Siemens Healthineers systems. NPS spatial frequencies were greater with MBIR than with H/SIR for Philips Healthcare (20 ± 2 [SD] %; range: 19—22%) and for Siemens Healthineers (9 ± 5 [SD] %; range: 4—14%) but lower for GE Healthcare (-17 ± 3 [SD] %; range: −14—−20%).

* Corresponding author.
E-mail address: joel.greffier@chu-nimes.fr (J. Greffier).

https://doi.org/10.1016/j.diii.2019.08.003

Conclusion: Using bone kernel with recent MBIR algorithms reduces the noise-magnitude for all CT systems assessed. Noise texture shifted towards high frequency for Siemens Healthineers and Philips Healthcare but the opposite for GE Healthcare.

Abbreviations

CNR	Contrast-to-noise ratio
CT	Computed tomography
FBP	Filtered back projection
GE	General Electric
H/SIR	Hybrid/statistical Iterative reconstruction
IR	Iterative reconstruction
MBIR	Model-based iterative reconstruction
NPS	Noise power spectrum
ROI	Region of interest

Introduction

Dose optimization is essential to reduce the doses delivered to the patient during computed tomography (CT) examination [1,2]. Several tools have been developed for dose reduction, including iterative reconstructions (IR). Several generations of IR algorithms are proposed by CT system manufacturers [3,4] such as hybrid or statistical IR (H/SIR) algorithms and model-based iterative reconstruction (MBIR) algorithms. H/SIR algorithms combine filtered back projection (FBP) and IRs in different proportions. Recent MBIR algorithms use a probabilistic method, taking into account the physically correct modulation of the data acquisition process (including system geometry and noise models) to effectively reduce noise and artifacts [5,6].

To assess the image quality with IR algorithms, new metrics such as the noise power spectrum (NPS) were used. As defined by Verdun et al., NPS gives a complete description of the noise by plotting the amplitude (noise-magnitude) according to the frequency of the image, which are known as noise-texture (e.g., image smoothing) [7].

A recent study assessed the noise-magnitude and noise-texture produced by two generations of algorithms of three manufacturers [8]. This study concluded that in comparison with the preceding generation, recent MBIR algorithms differ between main manufacturers with respect to noise-magnitude and noise-texture. However, this study was performed only for ''soft tissue'' kernel and in clinical practice; ''bone'' kernel was also used to assess the tissue and the structure of the bone. These two types of kernels have a different impact on image noise and spatial resolution. Compared to the strong kernel, the images obtained using a soft kernel have a lower noise level but a degraded spatial resolution. It is therefore important to assess the impact of each kernel on image quality in a dose optimization process.

The aim of this study was to compare the noise-magnitude and noise-texture produced by different IR algorithms with ''bone'' kernel according to the methodology used in a previous work carried out at our institution using ''soft'' kernel [8].

Materials and methods

Experimental procedure and CT systems

The same experimental procedure was performed on the same CT systems as those defined in a previous work carried out at our institution [8]. Five CT systems from three different manufacturers placed inside or outside our institution were used in this study.

Acquisitions of a Catphan 600 phantom (The Phantom Laboratory) were performed using a tube voltage of 120 kV. Tube currents (mA) were defined to obtain three different dose levels: 3.0, 7.0 and 12.0mGy.

Raw data were reconstructed with standard ''bone tissue'' reconstruction kernel and with the FBP and the intermediate iterative level of the two generations of IR algorithm (H/SIR and MBIR algorithms) available on each system and usually used in clinical practice. IR level and kernel for each CT system were defined with support of the application specialist of each manufacturer. Images were reconstructed with a field-of-view of 250 mm and a slice thickness close to 1 mm (1 mm increment).

Acquisition and reconstruction parameters for each CT system used are defined in Table 1.

Contrast-to-noise ratio (CNR)

Image quality evaluations were performed using in-house Matlab (MathWorks) routines. Two circular regions of interest (ROI) of 420 pixels (0.785 cm^2) were placed semi-automatically on the CTP 401 section in two inserts: Teflon (range from 941 to 1060 HU) and low-density polyethylene (LDPE; range from −121 to −87 HU) (Fig. 1a). The mean of CT number (average of pixels; N_{CT}) and the image noise (standard deviation of pixels) of the solid water (range from −7 to 7 HU) on the CTP 486 section were assessed by placing a ROI of 14400 pixels (36 cm^2) in the center of the phantom (Fig. 1b). The N_{CT} and image-noise were computed within each ROI in 15 consecutive reconstructed slices [9,10].

Table 1 Acquisition and reconstruction parameters used on each CT-scan.

Manufacturer	GE Healthcare		Philips Healthcare	Siemens Healthineers	
Model	Revolution® GSI	Revolution® Evo	Ingenuity® Elite	Definition® AS+	EDGE®
Location (in/outside our institution)	In	Outside	Outside	In	Outside
mAs values used according to the $CTDI_{vol}$					
12 mGy	290	270	184	178	178
7 mGy	170	160	107	104	104
3 mGy	70	70	46	45	45
Pitch	0.984		0.984	1	1
IR algorithm and IR level	Asir 50%	Asir-V 50%	iDose^4 3/IMR 2	SAFIRE 3	ADMIRE 3
Reconstruction kernel	Bone	Bone	YA/SharpPlus	I70	I70
Detector	Gemstone	Gemstone	Elite IMR Ready	Ultra Fast Ceramic	Stellar
Thickness/overlap	1.25 mm/1.25 mm		1 mm/1 mm	1 mm/1 mm	
Collimation	64 × 0.625 mm		64 × 0.625 mm	64 × 0.6 mm	

IR: Iterative reconstruction; ADMIRE advanced modeled iterative reconstruction; ASIR: adaptive statistical iterative reconstruction; $CTDI_{vol}$: volume computed tomography dose index; iDose: intelligent dose; IMR:iterative model reconstruction; SAFIRE: sinogram affirmed iterative reconstruction.

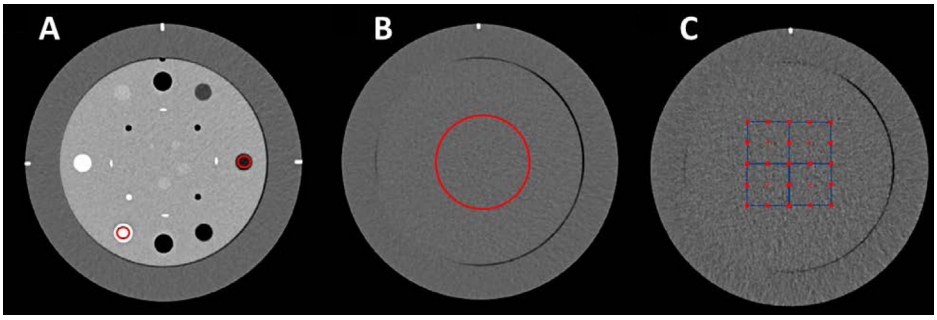

Figure 1. a: ROIs used to compute the N_{CT} and image noise of Teflon insert and LPDE insert (2.); b: ROI used to compute the N_{CT} and image noise of solid water; c: ROIs used for the Noise Power Spectrum assessment.

The contrast-to-noise ratio (CNR) between both inserts and the solid water was calculated as follows:

$$CNR = \frac{|HU_{insert} - HU_{water}|}{\sigma_{water}}$$

where HU is Hounsfield Unit.

For each manufacturer, CNR values were compared for FBP versus H/SIR, FBP versus MBIR, H/SIR versus MBIR and FBP versus FBP if two different CT scans were used.

Noise power spectrum

NPS were calculated with an in-house MATLAB® routine in the uniform section of Catphan phantom (CTP 406) as follows:

$$NPS_{2D}\left(f_x f_y\right) = \frac{\Delta_x \Delta_y}{L_x L_y} \frac{1}{N_{ROI}} \sum_{i=1}^{N_{ROI}} \left| FT_{2D}\left\{ ROI_i\,(x,y) - \overline{ROI_i} \right\} \right|^2$$

where Δ_x and Δ_y are the pixel size in x- and y-direction; L_x et L_y are the ROIs length in the x- and y-directions; N_{ROI} the number of ROI; FT the Fourier transform and $\overline{ROI_i}$ is the background or structured noise measured from ROI (x, y) using a first-order (subtraction of a 3D linear fit) detrending technique.

NPS was computed in a total of 80 ROIs, 64 × 64 pixels each, within 20 consecutive axial sections.

For each manufacturer, the values of NPS peak and NPS spatial frequency were compared for: FBP versus H/SIR, FBP versus MBIR, H/SIR versus MBIR and FBP versus FBP if two different CT scans were used.

Statistical analysis

Statistical analyses were performed using our in-house developed MATLAB routine (MathWorks, Natick, USA). Comparisons of CNR values between FBP and IR algorithms were performed using the Wilcoxon ranked sum non-parametric

test. *P*-values were corrected for multiple comparisons (Bonferonni test) and only values lower than 0.001 (*P* corrected < 0.001) were considered significant.

Results

Contrast-to-noise ratio

The CNR values for reconstructions with FBP, H/SIR and MBIR as function of the dose levels are shown in Fig. 2 and Table 2. For both inserts the CNR for FBP was lower than H/SIR or MBIR algorithms. These differences were significant for all CT-scans and inserts ($P < 0.001$). On average, CNR improved from FBP to H/SIR algorithms by 49 ± 1 [SD] % (range: 48—50%) for GE Healthcare, 29 ± 1 [SD] % (range: 28—30 %) for Philips and 26 ± 2 [SD] % (range: 23—28%) for Siemens Healthineers systems. In both inserts, CNR were significantly higher in FBP-Evo than FBP-GSI ($P < 0.001$) and in FBP-Edge than FBP-AS+ ($P < 0.01$). On average, CNR was improved by 37 ± 8 [SD] % (range: 29—49 %) for GE Healthcare and 11% ± 6 [SD] % (range: 3—17 %) for Siemens Healthineers systems.

For all systems, CNR was significantly higher with MBIR than with H/SIR ($P < 0.001$) and differences between both IR algorithms decreased when the dose increased.

Regarding GE Healthcare systems (Fig. 2a and b), CNR improved on average from ''Asir'' to ''Asir-V'' by 34 ± 13 [SD] % (range: 24—49 %) for Teflon insert and 38 ± 17 [SD] % (range: 24—57%) for LDPE insert.

With respect to Philips Healthcare system (Fig. 2c and d), CNR improved on average from ''iDose^4'' to ''IMR'' by 105 ± 19 [SD] % (range: 89—126 %) for Teflon insert and 113 ± 2 3% (range: 94—139 %) for LDPE insert.

Regarding Siemens Healthineers systems (Fig. 2e and f), CNR improved on average from ''SAFIRE'' to ''ADMIRE'' by 41 ± 6 [SD] % (range: 36—47 %) for Teflon insert and 42 ± 5 [SD] % (range: 38—47 %) for LDPE insert.

Noise power spectrum

NPS-peak

NPS peaks decreased as the dose increased, independently of the system and the reconstruction algorithms used (Table 3 and Fig. 3).

NPS peak with FBP was higher than with H/SIR or MBIR algorithms. The mean NPS peak decreased from FBP to H/SIR algorithms by −61 ± 0 [SD] % (range: −61—−60 %) for GE, −41 ± 0 [SD] % (range: −42—−41 %) for Philips Healthcare and −32 ± 2 [SD] % (range: −34—−30 %) for Siemens Healthineers systems. NPS peaks were lower in FBP-Edge than FBP-AS+ and in FBP-Evo than FBP-GSI. On average the NPS peak was decreased by −55 ± 2 [SD] % (range: −57—−53 %)

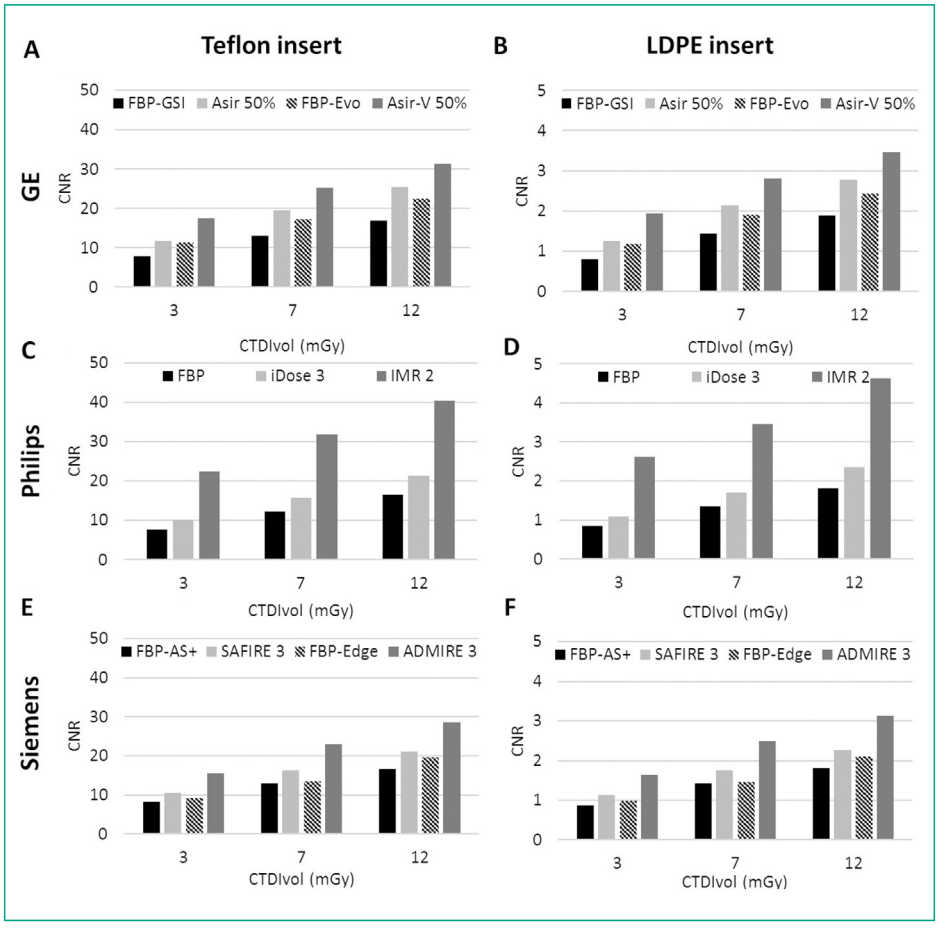

Figure 2. Mean values of contrast-to-noise ratio for Teflon and LDPE inserts as function of the dose levels for FBP, H/SIR and MBIR algorithms of three manufacturers.

Table 2 Contrast to noise ratio of Teflon and LDPE inserts obtained with bone kernels according to the dose level for each CT-scan and reconstruction type.

Manufacturer	Reconstruction type	CNR Teflon			CNR LDPE		
		3 mGy	7 mGy	12 mGy	3 mGy	7 mGy	12 mGy
GE Healthcare	FBP-GSI	7.9 (7.8; 7.9)	13.0 (12.9; 13.0)	16.9 (16.7; 16.9)	0.8 (0.8; 0.9)	1.4 (1.4; 1.4)	1.9 (1.9; 1.9)
	Asir 50%	11.7 (11.7; 11.8)	19.5 (19.4; 19.5)	25.3 (25.1; 25.4)	1.3 (1.2; 1.3)	2.1 (2.1; 2.1)	2.8 (2.8; 2.8)
	FBP-Evo	11.4 (11.3; 11.4)	17.2 (17.2; 17.3)	22.4 (22.2; 22.4)	1.3 (1.2; 1.3)	1.9 (1.9; 1.9)	2.5 (2.4; 2.5)
	Asir-V 50%	17.4 (17.3; 17.5)	25.2 (25.0; 25.2)	31.3 (31.1; 31.3)	2.0 (1.9; 2.0)	2.8 (2.8; 2.9)	3.5 (3.5; 3.5)
Philips	FBP	7.7 (7.6; 7.7)	12.3 (12.2; 12.3)	16.4 (16.4; 16.5)	0.8 (0.8; 0.9)	1.3 (1.3; 1.3)	1.8 (1.8; 1.9)
Healthcare	iDose^4 3	9.9 (9.9; 9.9)	15.8 (15.8; 15.8)	21.2 (21.2; 21.3)	1.1 (1.0; 1.1)	1.7 (1.6; 1.7)	2.4 (2.4; 2.4)
	IMR 2	22.4 (22.3; 22.4)	31.7 (31.7; 31.8)	40.1 (40.0; 40.2)	2.6 (2.5; 2.6)	3.4 (3.4; 3.5)	4.6 (4.6; 4.6)
Siemens	FBP-AS+	8.2 (8.2; 8.2)	13.0 (12.9; 13.0)	16.7 (16.7; 16.7)	0.9 (0.9; 0.9)	1.4 (1.4; 1.4)	1.8 (1.8; 1.8)
Healthineers	SAFIRE 3	10.5 (10.5; 10.5)	16.3 (16.3; 16.3)	21.1 (21.0; 21.1)	1.1 (1.1; 1.1)	1.8 (1.7; 1.8)	2.3 (2.3; 2.3)
	FBP-Edge	9.2 (9.1; 9.2)	13.5 (13.5; 13.6)	19.6 (19.6; 19.7)	1.0 (1.0; 1.0)	1.5 (1.4; 1.5)	2.1 (2.1; 2.1)
	ADMIRE 3	15.4 (15.4; 15.5)	22.9 (22.9; 23.0)	28.7 (28.5; 28.7)	1.6 (1.6; 1.7)	2.5 (2.5; 2.5)	3.1 (3.1; 3.2)

Values are expressed as median (1st quartile; 3rd quartile). ADMIRE: advanced modeled iterative reconstruction; ASIR: adaptive statistical iterative reconstruction; CNR: Contrast-to-noise ratio; FBP: Filtered back projection; iDose: intelligent dose; IMR: iterative model reconstruction; LDPE: low-density polyethylene; SAFIRE: sinogram affirmed iterative reconstruction.

Table 3 Noise power spectrum peak and spatial frequency obtained with bone kernels according to the dose level for each CT-scan and reconstruction type.

Manufacturer	Kernel	Reconstruction type	NPS peak ($HU^2.mm^2$)			NPS spatial frequency (mm^{-1})		
			3 mGy	7 mGy	12 mGy	3 mGy	7 mGy	12 mGy
GE Healthcare	Bone	FBP-GSI	4222	1730	1006	0.83	0.82	0.83
	Bone	ASIR 50 %	1662	690	392	0.82	0.79	0.79
	Bone	FBP-Evo	1936	736	476	0.66	0.71	0.69
	Bone	ASIR-V 50 %	878	404	253	0.69	0.68	0.63
Philips Healthcare	YA	FBP	7031	3041	1733	0.58	0.58	0.58
	YA	iDose^4 3	4089	1794	1022	0.58	0.58	0.58
	Sharp+	IMR 2	717	371	245	0.71	0.69	0.69
Siemens Healthineers	B70	FBP-AS+	7753	3405	1912	0.58	0.55	0.57
	I70	SAFIRE 3	5133	2375	1299	0.52	0.50	0.50
	B70	FBP-Edge	7377	3202	1803	0.57	0.57	0.58
	I70	ADMIRE 3	2536	1084	636	0.54	0.55	0.57

ADMIRE: advanced modeled iterative reconstruction; ASIR: adaptive statistical iterative reconstruction; FBP: Filtered-back projection; iDose: intelligent dose; IMR: iterative model reconstruction; LDPE: low-density polyethylene; NPS: Noise power spectrum; SAFIRE: sinogram affirmed iterative reconstruction.

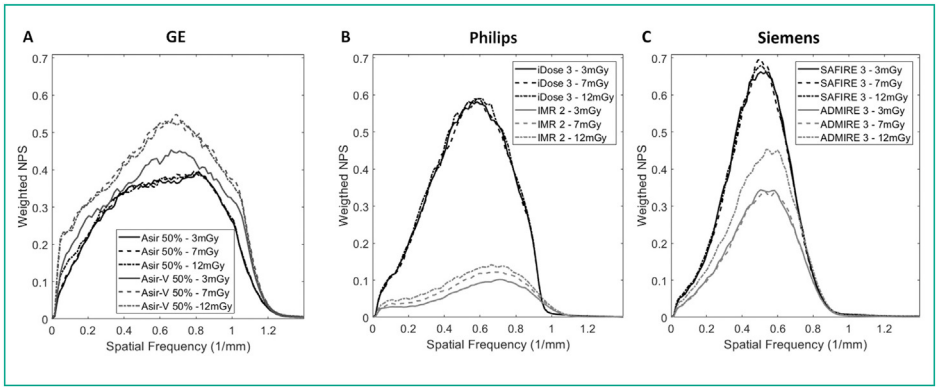

Figure 3. NPS curves weighted by NPS peak of FBP at each dose level (3, 7 and 12 mGy) for H/SIR and MBIR algorithms of three manufacturers.

for GE Healthcare and -6 ± 1 [SD] % (range: -6—-5 %) for Siemens Healthineers systems.

For all systems, NPS peaks were higher with H/SIR than with MBIR. The mean NPS peak decreased from H/SIR to MBIR by -41 ± 6 [SD] % (range: -47 —-35 %) for GE Healthcare, -79 ± 3 [SD] % (range: -82—-76 %) for Philips Healthcare and -52 ± 2 [SD] % (range: -54—-51 %) for Siemens Healthineers systems. For GE Healthcare and Philips Healthcare systems, differences between both IR algorithms decreased when the dose increased.

Noise-texture

Results of NPS spatial frequencies of IR algorithms are depicted in Table 3 and Fig. 3. Regarding GE Healthcare systems (Fig. 3.a), NPS spatial frequencies were higher in FBP-Evo (0.827 ± 0.006 [SD] mm^{-1}; range: 0.820 - 0.830 mm^{-1}) than FBP-GSI (0.687 ± 0.025 [SD] mm^{-1}; range: 0.660—0.710 mm^{-1}). The same outcomes were found between ''Asir'' (0.800 ± 0.017 [SD] mm^{-1}; range: 0.790—0.820 mm^{-1}) and ''Asir-V'' (0.667 ± 0.032 [SD] mm^{-1}; range: 0.630—0.690 mm^{-1}). Finally, NPS spatial frequencies were on average -17 ± 4 [SD] % (range: -20—-13 %) lower in FBP-Evo compared to FBP-GSI and on average -17 ± 3 [SD] % (range: -20—-14 %) lower in Asir-V compared to Asir.

With respect to Philips Healthcare system (Fig. 3b), values of NPS spatial frequency were in the same range between FBP (0.580 ± 0.001 [SD] mm^{-1}; range: 0.580—0.580 mm^{-1}) and ''iDose^4'' (0.580 ± 0.001 [SD] mm^{-1}; range: 0.580—0.580 mm^{-1}). NPS spatial frequencies were higher in ''IMR'' (0.697 ± 0.012 [SD] mm^{-1}; range: 0.690—0.710 mm^{-1}) than ''iDose^4''.

Regarding Siemens Healthineers systems (Fig. 3c), values of NPS spatial frequency were in the same range between FBP-AS+ (0.567 ± 0.015 [SD] mm^{-1}; range: 0.550—0.580 mm^{-1})] and FBP-Edge (0.573 ± 0.006 [SD] mm^{-1}; range: 0.570—0.580 mm^{-1}). NPS spatial frequency were lower with ''SAFIRE'' than with ''FBP-AS+'' (average -11 ± 2 [SD] % (range: -12—-9 %). Finally, NPS spatial frequencies were higher in ''ADMIRE'' (0.553 ± 0.015 [SD] mm^{-1}; range: 0.540—0.570 mm^{-1}) than ''SAFIRE'' (0.507 ± 0.012 [SD] mm^{-1}; range: 0.500—0.520 mm^{-1}).

Discussion

Image quality assessments in CT scan have usually been performed on reconstructed images using soft reconstruction kernel [8,11—16]. However, in clinical practice, reconstructed images using a bone kernel are mandatorily used for musculoskeletal studies and, depending on the institution policy, also on studies performed other than musculoskeletal purposes. To our knowledge, few studies have assessed the impact of bone reconstruction kernel on noise properties according to IR algorithms. For the first time, this phantom study assessed the noise-magnitude and noise-texture for both generations of IR algorithm proposed by three CT vendors using bone reconstruction kernel.

Our results showed that CNR values were improved with both generations of IR algorithms compared to FBP and with MBIR compared to H/SIR. Similar outcomes were found using the soft kernel for GE Healthcare and Philips Healthcare systems [8]. However, the opposite pattern was observed for Siemens Healthineers systems. For soft kernel, the CNR was reduced with ''ADMIRE'' compared to ''SAFIRE'' (-4 ± 5 [SD] %) [8], while CNR was improved using bone kernel (42 ± 5 [SD] %). This outcome showed that ADMIRE had a stronger impact on noise reduction and also on CNR improvement when strong kernel was used compared to soft kernel. It should also be noted that the same CNR variations with FBP between both GE Healthcare systems and both Siemens Healthineers systems were found for soft or bone kernels.

Our results showed that noise-magnitude was reduced with both generations of IR algorithms compared to FBP and with MBIR compared to H/SIR for all CT systems. NPS peak variations between MBIR and H/SIR were in the same range for bone and soft kernel for GE Healthcare (-42 ± 8 [SD] % for soft kernel and $-41\% \pm 6$ [SD] % for bone kernel) and Philips Healthcare (-75 ± 4 [SD] % for soft kernel and -79 ± 3 [SD] % for bone kernel) systems. As for CNR, the opposite pattern was observed for Siemens Healthineers systems. For soft kernel, the NPS peak was increased with ''ADMIRE'' compared to ''SAFIRE'' (13 ± 11 [SD] %) [8], while NPS peak was reduced using bone kernel (-52 ± 2 [SD] %).

Our results for noise-texture confirmed the results found using soft kernel for Siemens Healthineers and GE Healthcare systems. Using MBIR compared to H/SIR, the NPS spatial frequency shifted towards high frequencies for Siemens Healthineers whereas it displaced toward low frequencies for GE Healthcare. For Philips Healthcare system, different results were observed according to the kernel. For soft kernel, the NPS spatial frequency shifted towards low frequency [8] whereas it displaced towards high frequencies using bone kernel. It should also be noted that the results of NPS spatial frequencies with FBP were different between the two GE Healthcare systems assessed.

Finally, we observed that the use of MBIR compared to H/SIR showed better results on the metrics studied with bone kernel than with the soft kernel for Siemens Healthineers and Philips Healthcare. For Siemens Healthineers, the noise-magnitude was reduced with MBIR for strong kernel, which leads to reduced image-noise and thus improves the CNR. For Philips Healthcare, shifting the NPS peak to higher frequencies resulted in a decrease in image smoothing that was strongly present with IMR on soft kernel images [8]. For GE Healthcare, the impact on the metrics studied was the same between both kernels.

In the present study, the same limitations apply as those defined previously by Greffier et al. for the soft kernel [8]. Briefly, raw-data were reconstructed using one iterative level; the effect of the two generations of IR algorithm on spatial resolution and on detectability indexes was not assessed and the assessment of noise-texture and noise-magnitude was performed on two different CT systems for GE Healthcare and Siemens Healthineers. Finally, the results found in this phantom study need to be confirmed in patients by radiologists.

In conclusion, this phantom study performed with a bone reconstruction kernel and an intermediate iterative level suggested that features of the recent MBIR algorithms compared to the preceding generation differ compared to the previous results using soft reconstruction kernel. The noise-magnitude was reduced for all CT systems. The noise-texture shifted towards high frequencies for Siemens Healthineers and Philips Healthcare but the opposite for GE Healthcare.

Funding

This work did not receive any grant from funding agencies in the public, commercial, or not-for-profit sectors.

Author contributions

All authors attest that they meet the current International Committee of Medical Journal Editors (ICMJE) criteria for Authorship.

Acknowledgements

We would like to thank Dr J.M. Teissier for giving us permission to use the results of these measurements. We thank F. Mahinc for his support in this study. We thank S. Kabani for her help in editing the manuscript. We thank C. Demattei for his statistical support.

Disclosure of interest

The authors declare that they have no competing interest.

References

[1] Kalra MK, Maher MM, Toth TL, Hamberg LM, Blake MA, Shepard JA, et al. Strategies for CT radiation dose optimization. Radiology 2004;230:619—28.
[2] Gunn ML, Kohr JR. State of the art: technologies for computed tomography dose reduction. Emerg Radiol 2010;17:209—18.
[3] Patino M, Fuentes JM, Hayano K, Kambadakone AR, Uyeda JW, Sahani DV. A quantitative comparison of noise reduction across five commercial (hybrid and model-based) iterative reconstruction techniques: an anthropomorphic phantom study. AJR Am J Roentgenol 2015;204:W176—83.

[4] Viry A, Aberle C, Racine D, Knebel JF, Schindera ST, Schmidt S, et al. Effects of various generations of iterative CT reconstruction algorithms on low-contrast detectability as a function of the effective abdominal diameter: a quantitative task based phantom study. Phys Med 2018;48:111—8.
[5] Willemink MJ, Noel PB. The evolution of image reconstruction for CT-from filtered back projection to artificial intelligence. Eur Radiol 2019;29:2185—95.
[6] Verdun FR, Racine D, Ott JG, Tapiovaara MJ, Toroi P, Bochud FO, et al. Image quality in CT: From physical measurements to model observers. Phys Med 2015;31:823—43.
[7] Thibault JB, Sauer KD, Bouman CA, Hsieh J. A three-dimensional statistical approach to improved image quality for multislice helical CT. Med Phys 2007;34:4526—44.
[8] Greffier J, Larbi A, Frandon J, Moliner G, Beregi JP, Pereira F. Comparison of noise-magnitude and noise-texture across two generations of iterative reconstruction algorithms from three manufacturers. Diagn Interv Imaging 2019;100:7—8.
[9] Samei E, Richard S. Assessment of the dose reduction potential of a model based iterative reconstruction algorithm using a task-based performance metrology. Med Phys 2015;42:314—23.
[10] Aurumskjold ML, Ydstrom K, Tingberg A, Soderberg M. Improvements to image quality using hybrid and model-based iterative reconstructions: a phantom study. Acta Radiol 2017;58:53—61.
[11] Greffier J, Macri F, Larbi A, Fernandez A, Khasanova E, Pereira F, et al. Dose reduction with iterative reconstruction: optimization of CT protocols in clinical practice. Diagn Interv Imaging 2015;96:477—86.
[12] De Marco P, Origgi D. New adaptive statistical iterative reconstruction ASiR-V: assessment of noise performance in comparison to ASiR. J Appl Clin Med Phys 2018;19:275—86.
[13] Solomon JB, Christianson O, Samei E. Quantitative comparison of noise texture across CT scanners from different manufacturers. Med Phys 2012;39:6048—55.
[14] Ott JG, Becce F, Monnin P, Schmidt S, Bochud FO, Verdun FR. Update on the non-prewhitening model observer in computed tomography for the assessment of the adaptive statistical and model-based iterative reconstruction algorithms. Phys Med Biol 2014;59:4047—64.
[15] Si-Mohamed S, Greffier J, Bobbia X, Larbi A, Delicque J, Khasanova E, et al. Diagnostic performance of a low dose triple rule-out CT angiography using SAFIRE in emergency department. Diagn Interv Imaging 2017;98:881—91.
[16] Greffier J, Frandon J, Larbi A, Beregi JP, Pereira F. CT iterative reconstruction algorithms: a task-based image quality assessment. Eur Radiol 2019;29:1—14.